

Published in final edited form as:

J Vis. ; 12(11): . doi:10.1167/12.11.8.

Does optic flow parsing depend on prior estimation of heading?

Paul A. Warren,

School of Psychological Sciences, The University of Manchester, Manchester, UK,
Paul.Warren@manchester.ac.uk

Simon K. Rushton, and

School of Psychology, Cardiff University, Cardiff, UK, rushtonsk@cardiff.ac.uk

Andrew J. Foulkes

School of Psychological Sciences, The University of Manchester, Manchester, UK,
andrew.foulkes@manchester.ac.uk

Abstract

We have recently suggested that neural *flow parsing* mechanisms act to subtract global optic flow consistent with observer movement to aid in detecting and assessing scene-relative object movement. Here, we examine whether flow parsing can occur independently from heading estimation. To address this question we used stimuli comprising two superimposed optic flow fields comprising limited lifetime dots (one planar and one radial). This stimulus gives rise to the so-called optic flow illusion (OFI) in which perceived heading is biased in the direction of the planar flow field. Observers were asked to report the perceived direction of motion of a probe object placed in the OFI stimulus. If flow parsing depends upon a prior estimate of heading then the perceived trajectory should reflect global subtraction of a field consistent with the heading experienced under the OFI. In Experiment 1 we tested this prediction directly, finding instead that the perceived trajectory was biased markedly in the direction opposite to that predicted under the OFI. In Experiment 2 we demonstrate that the results of Experiment 1 are consistent with a positively weighted vector sum of the effects seen when viewing the probe together with individual radial and planar flow fields. These results suggest that flow parsing is not necessarily dependent on prior estimation of heading direction. We discuss the implications of this finding for our understanding of the mechanisms of flow parsing.

Keywords

optic flow processing; heading; flow parsing; object movement; ego-motion

Introduction

Retinal motion of images of objects in the scene can result from observer movement (Figure 1A), object movement (Figure 1B), or some combination of the two (Figure 1C). This raises a difficult problem for the brain of a moving observer to work out which components of the retinal motion arise from movement of objects in the scene. Essentially the brain needs to separate (or parse) the retinal motion field into its causal components. How might the brain achieve this?

© 2012 ARVO

Correspondence to: Paul A. Warren.

Commercial relationships: none.

One solution to this problem involves the use of nonvisual information about self movement. Investigations conducted by von Holst and Mittelstaedt (1950) and Sperry (1950) suggest that copies of the motor commands driving observer movement (efference copy) are generated in the central nervous system and used to cancel the sensory input arising due to observer movement. Similarly, other nonvisual information sources about observer movement, such as vestibular signals and proprioception, could also contribute to the cancellation process (e.g., see Donaldson, 2000).

In addition to the nonvisual solution, several investigators have suggested that a purely visual mechanism might also play a role in the assessment of object movement during observer movement (Bravo, 1998; Royden, Wolfe, & Klempen, 2001; Rushton & Warren, 2005). A visual solution is necessary because circumstances exist in which nonvisual information (efference copy and both vestibular and proprioceptive signals) provides unreliable, inappropriate, or noisy information about observer movement (Warren & Rushton, 2009a). For example, consider a passenger in a car travelling at a constant speed of 70 miles per hour. Efference copy and proprioceptive information would signal that the observer is staying relatively still and vestibular information would be limited due to the constant velocity movement. However, the observer is moving rapidly through the environment and, consequently, experiencing a complex optic flow field which must be disentangled to assess how other objects are moving in the scene.

Although the simple example given above indicates the need for a visual solution, compelling evidence for the existence of such a solution has only recently been reported (Rushton & Warren, 2005; Rushton, Bradshaw, & Warren, 2007; Warren & Rushton 2007; Warren & Rushton, 2008; Matsumiya & Ando, 2009; Warren & Rushton 2009a, 2009b; Royden & Connors, 2010; Calabro, Soto-Faraco, & Vaina, 2011).

In particular, our work has put forward the *flow parsing hypothesis* (Rushton & Warren, 2005; Rushton, Bradshaw, & Warren, 2007; Warren & Rushton, 2007; Warren & Rushton, 2008; Warren & Rushton, 2009a, 2009b). Under this hypothesis the brain uses visual information about self movement in the form of optic flow to assess scene-relative object movement. Briefly, the flow parsing hypothesis suggests that the brain is able to perform something akin to a global subtraction of the optic flow arising due to observer movement.

For example, consider the scene in Figure 2 in which an observer walks forwards down a corridor whilst a ball falls downwards under the influence of gravity. The left panel of Figure 2 demonstrates the problem: Due to the combination of self-generated and object-generated movement the retinal trajectory of any object in the scene is not necessarily indicative of the world-relative movement of that object. The center panel of Figure 2 provides a conceptual illustration of the operation proposed under flow parsing. It shows a cancellation field to be applied to the left panel if the observer were able to perfectly discount (subtract off) the self movement component of optic flow. The right panel of Figure 2 shows the perceived scene motion if the global subtraction process underpinning flow parsing were perfect. The motion signals remaining after the subtraction would be comparable to those which would be present if the observer was stationary in the scene.

The flow parsing hypothesis has been tested repeatedly in a number of paradigms (Rushton & Warren, 2005; Rushton, Bradshaw, & Warren, 2007; Warren & Rushton 2007; Warren & Rushton, 2008; Warren & Rushton, 2009a, 2009b). Perhaps the most compelling demonstration of the global subtraction process at work is found in Warren and Rushton (2009a). In this study, stationary observers viewed limited lifetime dot motion displays consistent with forwards translation through a cloud of dots (a radial optic flow field). In addition observers saw a probe on the screen moving horizontally at 2° or 4° above fixation.

Under the flow parsing hypothesis it was predicted that the radial expansion field should be globally subtracted from the retinal motion field. At the location of the probe this corresponds to subtraction of the blue vector shown in Figure 3. Subtraction of the blue vector is equivalent to addition of the magenta vector in Figure 3 and consequently the perceived trajectory of the probe is predicted to tilt inwards towards the center (focus of expansion, FOE) of the radial flow field (Figure 3). A second prediction of the flow parsing account was that the size of the tilt effect should increase with probe eccentricity, because in a radial flow field motion vectors further from the focus of expansion tend to be larger (Figure 3) and so the component to be subtracted should also be larger. A third prediction suggested that, due to the global nature of the subtraction process, the first two predictions would still hold even if the radial flow information was removed in the hemi-field containing the probe. It is worth emphasizing the strength of this prediction since it leads to the very counterintuitive claim that when the probe is moved further away from the hemi-field containing the radial flow stimulus, the illusory tilt inwards should increase. The results of Warren and Rushton (2009a) confirmed all these predictions. Taken together with independent evidence from other investigators (Matsumiya & Ando, 2009; Royden & Connors, 2010; Calabro, Soto-Faraco, & Vaina, 2011) these studies put forward a compelling case for the existence of a visual optic flow parsing mechanism which supports the estimation of scene-relative object movement.

The flow parsing hypothesis provides a novel role for optic flow processing in the human brain. A large body of earlier research, inspired primarily by the work of Gibson (1950), has focused instead on the ability of observers to estimate *heading*, the instantaneous direction of self-movement, from optic flow fields. It has been demonstrated that observers can estimate heading from optic flow information to within a degree or two (Warren, Morris, & Kalish, 1988) in less than 150 ms (van den Berg, 1992).

Given that flow parsing and heading estimation both rely upon processing of optic flow to recover information about self movement, an obvious question is whether there is a relationship between these mechanisms. Is flow parsing dependent on a prior estimate of heading direction or are the two processes and associated judgments independent?

In this paper we exploit an interesting illusory heading phenomenon called the optic flow illusion (OFI; Duffy & Wurtz, 1993) to investigate these questions. The optic flow illusion arises when a planar flow field (consistent with eye, or to a first approximation, head rotation) is superimposed onto a radial flow field (consistent with forwards observer translation) (Figure 4A). In such circumstances observers typically report that the perceived heading direction (and perceived FOE of the radial flow field) is shifted in the same direction as the planar flow (Figure 4C). This is a surprising result since the effect is in the opposite direction to that predicted if the brain performed an addition or averaging operation on the overlapping vector flow fields, as might be expected intuitively (Figure 4B). In fact the commonly perceived effect illustrated in Figure 4C appears to be more consistent with subtraction of the planar field from the radial field.

If flow-parsing is dependent on a prior estimate of heading then we might expect perceived trajectory of a probe object presented within the OFI stimulus to also be susceptible to the illusion. Consequently we would expect perceived object trajectory to reflect global subtraction of the flow field associated with the OFI (Figure 4C). We tested this prediction in a series of experiments.

In a Preliminary experiment we measured the size of the OFI illusion for the stimuli used in the present study. The primary reason for doing this was to ensure that the basic stimulus used here did give rise to the OFI and to establish the approximate magnitude of the effect.

In the main experiment (Experiment 1) we test whether perceived trajectory of a probe presented in the OFI stimulus is susceptible to the OFI. The stimuli in Experiment 1 and possible outcomes are shown schematically in Figure 5. The basic manipulations are seen in the left panel of Figure 5A. Observers viewed stimuli comprising overlaid radial and planar flow fields together with a single probe object moving upwards at one of two possible onscreen locations. The right panel of Figure 5A shows the predictions for perceived trajectory of the probe if flow-parsing is susceptible to the OFI. If the flow parsing and heading estimation mechanisms were not independent then, due to the shift in perceived heading under the OFI, we would expect the trajectory to exhibit a commensurate tilt towards the illusory FOE. Alternatively, the middle panel of Figure 5A shows the predictions if the flow-parsing effect seen is, instead, more compatible with prior vector addition of the flow fields comprising the OFI stimulus. In this case we would expect the perceived probe trajectory to tilt towards the FOE obtained under vector addition.

In Figures 5B and C we show hemi-field versions of the stimulus in Figure 5A together with associated predictions. These conditions were added to explicitly test that the effects seen are not dependent on the presence of local motion information surrounding the probe. Flow parsing is a global process and, based on Warren and Rushton (2009a), we would expect to find a similar (but reduced in magnitude) pattern of responses when only a hemi-field is present, even when the probe and background motion are on opposite sides of the display.

In Experiment 2 we decompose the flow fields seen in Experiment 1 so that observers reported perceived probe trajectory when it was presented amidst the individual radial and planar optic flow fields. This allowed us to assess directly whether the effects seen in Experiment 1 could be described as a linear combination of effects found for the individual flow fields.

To anticipate the results, we demonstrate that, when presented together with the superimposed flow fields of the OFI, participants perceive the probe to move in a manner that is not consistent with prior estimation and use of heading (i.e., not consistent with the predictions in the right panels of Figure 5). We also find that the pattern of effects obtained in Experiment 1 is well approximated by a positively weighted vector sum of the effects seen in Experiment 2 for the individual flow fields comprising the OFI stimulus. This result is consistent with the idea that the perceived trajectory seen in Experiment 1 is based on vector field addition rather than subtraction (i.e., consistent with the predictions in the middle panels of Figure 5).

General methods

Participants

Five observers took part in the Preliminary experiment. Nine observers took part in Experiment 1 and the same nine took part in Experiment 2. All participants worked or studied in the School of Psychological Sciences, University of Manchester. Two of the authors were among the participants in all three studies (PAW and AJF); all other participants were naive regarding the purpose of the study. All participants had normal or corrected to normal vision. Recruitment and testing procedures were in line with the Declaration of Helsinki and were approved by the appropriate institutional ethics committees.

Apparatus

Observers were seated with the chin positioned in a chin rest in a dark room with the eyes at a distance of approximately 57 cm from the display. All stimuli were displayed on a 22 Viewsonic (pf225) CRT running at 100Hz with resolution 1024×768 pixels. The visible

portion of the CRT subtended approximately $40^\circ \times 30^\circ$. The CRT casing and edges of the visible portion of the screen were obscured by irregularly shaped black card. This minimized stray light reflecting from the casing. Experiments and stimuli were coded using Lazarus, a free open source development system for Pascal (<http://www.lazarus.freepascal.org/>) together with the JediSDL libraries which facilitate use of OpenGL in Pascal (<http://jedi-sdl.pascalgamedevelopment.com/>).

Stimuli

Stimuli in all three experiments were onscreen for 2 s and comprising either two overlapping (Preliminary experiment and Experiment 1) or individual (Experiment 2) optic flow fields composed of approximately 180 dots of constant radius (0.1°) and limited lifetime (25 frames = 250 ms). Flow fields were presented in a circular aperture which subtended approximately 20° . At generation and regeneration (i.e., when lifetime had expired), 2D onscreen dot location in both flow fields was sampled randomly from a uniform distribution and then assigned a random depth in the range 0.5–1.5 m from the observer before perspective back-projection to obtain a 3D location. Dot density was approximately 0.25 dots/deg².

In the first component flow field dots moved radially in a manner consistent with forward movement of an observer at 0.59 m/s through the dot cloud. Median onscreen dot speed was around 6° /s. The second component flow field was planar with all dots moving in the same direction at the same speed consistent with an eye (or to a first approximation head) rotation of approximately 5.7° /s. Given the viewing distance of 57.3 cm, onscreen dot speed was approximately 5.7° /s. The speed of the planar flow field was chosen to approximately match mean velocity in the radial flow field but no attempt was made to match velocities exactly. In some conditions the flow stimuli were present in the whole field; in others they were present in only one hemi-field (see design for details).

In Experiments 1 and 2, as well as the flow field(s), a small (0.09° diameter) probe dot was present in the display (Figure 5). The dot moved at approximately 0.6° /s on a linear trajectory. The trajectory direction was varied from trial to trial about vertical (see design for details) so that participants could never be sure whether perceived motion was real, illusory, or a combination of the two. The dot start position was at one of two locations 3° to the left or right of fixation (see design for details).

In all three experiments a fixation spot was presented at the center of the screen and participants were instructed to maintain fixation throughout the presentation of the flow field.

Preliminary experiment

Rationale

In the Preliminary experiment we measured the size of the OFI illusion for the stimuli used in the present study. The primary reason for doing this was to ensure that the stimulus used in the present experiments did give rise to the OFI. Obtaining an estimate of the perceived FOE for the stimulus used here is also useful since we can then make predictions based on the position of the probe relative to the perceived FOE.

We also measured the size of the OFI when only one hemi-field of the stimulus was presented. This was important because we placed the probe in a hemi-field of the OFI stimulus in some conditions of Experiment 1.

Design

In the Preliminary experiment we manipulated the structure of the field in two conditions so that either the OFI stimulus was present in the full field, or it was presented only in one hemi-field. We measured the direction of the perceived heading. Participants saw each condition 90 times, leading to 180 trials in total over two sessions. In addition the direction of the planar flow field varied randomly between left and right from trial to trial (we averaged results over this random factor—see section headed Data processing and analysis).

Procedure

After viewing the OFI stimulus, a small green dot appeared (0.3° diameter) and participants adjusted its horizontal position by moving the mouse to indicate the perceived direction of heading. When they were happy with the setting participants clicked the mouse and saw the next trial.

Data processing and analysis—On each trial the direction of the planar flow was randomly assigned as left or right. This random factor was eliminated at the analysis stage by flipping the sign of data in the leftward planar flow conditions. This is conceptually equivalent to reflecting the condition and data about a vertical axis through the center of the stimulus. Consequently, data are presented as if all trials had planar flow moving rightward.

Results

Results for the Preliminary experiment are presented in Figure 6. The predicted pattern of results found in the OFI is replicated with a small but reliable shift (of around 2° – 3°) in perceived heading direction in the same direction as the planar flow (positive errors are in the direction of the planar flow). Note that the effect persists (although the between subjects variability in the effect increases) in the hemi-field condition, a result which has been shown previously (Duijnhouwer, Beintema, van den Berg, & van Wezel, 2006).

One sample t tests (one-tailed) were undertaken to assess whether the OFI effect was different from zero across observers. These tests revealed that the observed perceived heading direction was significantly different from zero for the full field condition, $t(4) = 3.637$, $p < 0.01$, one-tailed, and marginally so for the hemi-field condition, $t(4) = 2.095$, $p = 0.06$, one-tailed. Furthermore a repeated measures t test revealed no evidence for a significant difference between the effects seen in the two field conditions, $t(4) = -0.11$, $p = 0.92$, two-tailed.

Experiment 1

Rationale

The purpose of Experiment 1 was to test whether the perceived trajectory of a probe presented in the OFI stimulus is susceptible to the OFI. If it is then we would expect a characteristic pattern of perceived probe trajectory (Figure 5, right hand column). Obtaining this pattern of results would, at least, be compatible with the idea that the mechanisms of flow parsing depend upon an estimate of heading.

Design

In Experiment 1 we manipulated three experimental factors (see Figure 5)—flow field structure with three levels (full field, left hemi-field, right hemi-field), probe direction with three levels (75° , 90° , 105°) and probe position with two levels (-3° , 3°). The planar flow field was always presented in the rightwards direction (consistent with a leftwards eye or, to a first approximation, head rotation). Crucially, we use similar manipulations to those in

Warren and Rushton (2009a) to control the influence of local and global motion processing mechanisms. When the probe is in the opposite hemi-field to the flow then it is at least 3° from the nearest moving dot in the background, thereby limiting the impact of local motion contrast processing mechanisms (e.g., Frost & Nakayama, 1983) on perceived trajectory. Any effect observed is likely then to be due to a global mechanism such as flow parsing. Conversely, when the probe is in the same hemi-field as the flow fields there is no constraint imposed on the distance between the probe and dots in the background so local motion contrast mechanisms may also impact upon the percept.

We measured perceived probe direction (see Procedure section) and relative tilt, defined as the difference between the actual and perceived probe directions (Figure 7). Participants saw each condition eight times giving 144 trials in total.

Procedure

After viewing the stimulus, observers saw onscreen an adjustable paddle together with reference horizontal and vertical axes (Figure 7). Participants were instructed to adjust the orientation of the paddle by moving the mouse until it matched the perceived orientation of the trajectory of the probe dot. Observers were explicitly told that in the rare event that they did not see the probe moving along a linear trajectory (e.g., if it appeared to curve) they should orient the paddle so that it provided a “best straight line fit” to the perceived trajectory.

Data processing and analysis—The relative tilt (RT) is defined as $RT = (\theta_p - \theta_R)$, where θ_p and θ_R are, respectively, the perceived (P) and real (R ; onscreen) probe trajectories (with 0° at the positive x -axis and increasing in an anticlockwise direction) (Figure 7). To make the data consistent across probe direction conditions, relative tilts obtained in the 75° and 105° probe angle conditions were transformed to the equivalent quantity \hat{RT} which would have been obtained if the probe had moved vertically using Equation 1 (see Warren & Rushton, 2007, for a derivation):

$$\hat{\theta}_{RT} = \tan^{-1}(\sin\theta_{RT}/\sin\theta_p). \quad (1)$$

In practice this manipulation makes a relatively small change to the relative tilt values obtained. Once this manipulation was undertaken we averaged over probe angle conditions.

In line with Warren and Rushton (2009a) data were relabeled based on stimulus type. Specifically, the hemi-field conditions were reclassified as four new stimulus types composed of different combinations of the possible stimulus conditions (see the stimuli and tables in left panels of Figure 5). In two of these conditions, referred to as the same type conditions (Figure 5B—left half of left panel and Figure 5C—right half of left panel), the probe and flow field were in the same hemi-field—these arise from the original conditions: (field left hemi-field, probe position = -3°) and (field right hemi-field, probe position = 3°). In the other two conditions, referred to as the opposite type conditions (Figure 5B—right half of left panel and Figure 5C—left half of left panel), the probe and flow field were in opposite hemi-fields—these arise from the original conditions: (field = left hemi-field, probe position = 3°) and (field = right hemi-field, probe position = -3°). In the remaining two conditions (field = full field, probe position = 3°) and (field = full field, probe position = -3°), the OFI stimulus is present in the whole field and we refer to these conditions as the both type since the flow is present both in the same hemi-field as, and the opposite hemi-field to, the probe.

Similar to Warren and Rushton (2009a), the relabeling enables us to test hypotheses about mechanisms which are either local (such as local motion contrast—see Frost & Nakayama, 1983) or global (such as optic flow parsing) in scope and which might contribute to the relative tilt effects seen. When the probe is in the opposite hemi-field to the flow fields then it is at least 3° from the nearest moving dot in the background, thereby limiting the impact of local motion contrast processing mechanisms on perceived trajectory. Conversely when the probe is in the same hemi-field as the flow fields there is no constraint imposed on the distance between the probe and dots in the background so local motion contrast mechanisms may impact upon the percept. Consequently, in the same type conditions and the both type conditions we expect that the results will be similar since (a) the local motion information is similar in these cases and (b) we assume that the hemi-field of flow should be sufficient to engage global processing of optic flow as if the full field stimulus were present (see Figures 5B and C). However, in the opposite conditions the probe and flow are in different hemi-fields and so although global motion processing mechanisms (such as flow parsing) should still be engaged there should be no (or at least a greatly reduced) contribution from local motion processing. Specifically, we would expect that the results in the opposite type conditions should be qualitatively similar to those seen in the both type conditions, although reduced in magnitude due to the loss of contributions from local motion processing (see Figures 5B and C).

Results

Figure 8 shows average relative tilt for the composite observer obtained by averaging over the nine participants. Data are shown for the full, same, and opposite type conditions when the probe was on the left and right hand side of the field. A schematic illustration of the conditions together with a graphical representation of the effects (orientation of red arrow relative to vertical) is also provided at the top of the plot.

Comparing the data to the predictions in Figure 5 (red arrows with dotted white outline in middle and right hand columns) we see that it is at odds with those made if flow parsing occurred only after heading estimation (Figure 5, right column). If flow parsing were undertaken based upon the heading recovered under the OFI then the relative tilt observed when the probe was in the right hemi-field should be considerably smaller than that obtained when the probe was in the left hemi-field. Instead, across all conditions, when the probe is in the right hemi-field its trajectory is perceived to tilt markedly to the left relative to the onscreen trajectory. In contrast when the probe is on the left side of the field, the size of the effect is reduced, a result confirmed by finding a main effect of probe position in a two-factor repeated measures ANOVA conducted on the absolute value of the effects in Figure 8, $F(1, 8) = 19.8$, $p = 0.002$. This pattern of effects is more consistent with the prediction made based on vector addition of the overlaid flow fields in the OFI stimulus (Figure 5, middle panel).

The hemi-field manipulation is seen to have a similar effect on results as in previous studies (e.g., Warren & Rushton, 2009a). Although there was little difference between the effects seen in the both and same condition types, the effects in the opposite condition types are reduced (although still significantly greater than zero when the probe was in the right hemi-field—95% $CI = [3.6, 17.1]$). These results suggest that although some of the effect seen in the full field condition is driven by a local process, there is a significant portion which is due to global processing of the kind expected under flow parsing. This result is supported by a main effect of field structure, $F(2, 16) = 12.3$, $p < 0.001$.

As noted above, the pattern of effects seen in this experiment is more consistent with the prediction made based on vector addition of the overlaid flow fields in the OFI stimulus (Figure 5, middle panel). In the next experiment we will test this suggestion in more detail.

Eye movement control

Several researchers have noted that optic flow stimuli can elicit eye movements (e.g., Miles, Kawano, & Optican, 1986; Lappe, Pekel, & Hoffman, 1998; Niemann, Lappe, Büscher, & Hoffman, 1999). Consequently, it is at least possible that either voluntary or involuntary eye movements could have produced the pattern of data presented in Figure 8. Under this account the relative tilts seen might be generated by horizontal eye movements, either predominantly to the right or left, to generate anticlockwise or clockwise relative tilts, respectively. We would argue that this is unlikely to explain the effects seen in our experiments. Even if our participants did ignore the instruction to fixate at the center of the screen, there is no reason why they should produce different eye movements depending on whether the probe was on the left- or right-hand side of the screen (as would be required to predict the data obtained).

In order to rule out the possibility that these data were due to eye movements, we have conducted a follow up study. We repeated Experiment 1 with five observers and measured eye position throughout each trial at 1000 Hz using an EyeLink 1000 eye-tracking system (SR Research). Eye-tracking methods were similar to those used in Champion and Freeman (2010) (see Supplementary Materials for more details).

In the follow-up experiment, the mean deviation from fixation per trial over all conditions and observers was relatively small—around 0.3° (18 arcmin) or 10% of the distance to the probe from fixation—and was similar across flow field and probe position conditions. In addition, there was little difference between the horizontal and vertical deviations from fixation. This is at odds with what we would expect if the relative tilt effects were driven by horizontal eye movements since we should then expect these to be larger than any random fluctuations in vertical eye position. These observations were confirmed in a three-factor (Probe Position \times Flow Field Structure \times Direction of Deviation) repeated measures ANOVA revealing no main effects of or interactions between factors ($p > 0.175$ in all cases) (see Supplementary Materials for more detail). In addition, the pattern of relative tilt data obtained was very similar to that seen in Figure 8 (see Supplementary Materials). Finally, when a strict constraint was imposed on allowable deviations from fixation such that trials on which this exceeded 0.25° (15 arcmin) were excluded, the relative tilt data were also similar to Figure 8 (see Supplementary Materials).

In the Supplementary Materials we have also provided average (over observer and repetitions) eye-movement traces for each of the six (Field Structure \times Probe Position) conditions. There is no evidence for any systematic pattern of eye movements in these traces that would predict the results seen.

Considering the observed accuracy of fixation in our follow-up experiment, the lack of difference between vertical and horizontal deviations from fixation, and the lack of a systematic pattern of eye movements that might predict the relative tilt effects seen, the movements observed in our follow up study are likely to represent nonsystematic random fluctuations in eye position. Consequently, although it is of course possible that eye movements could contribute a small component to the effects seen, we are confident that our results are not based upon unwanted oculomotor effects.

Experiment 2

Rationale

In Experiment 1 the pattern of relative tilt effects seen was not consistent with what might be expected if flow parsing occurred only after the heading was estimated. Instead the data

were more consistent with global subtraction of the vector sum of the flow fields comprising the OFI stimulus. In Experiment 2 we examine this possibility more closely.

We investigated whether the results of Experiment 1 could be modeled as a simple weighted linear combination of effects found when viewing the probe together with the individual components of the OFI field. We reasoned that by examining the fitted weights for the individual components we could assess whether the effects in Experiment 1 were most consistent with global subtraction of either a vector sum or vector difference (radial minus planar) of the flow fields comprising the OFI stimulus.

Design

In Experiment 2 we manipulated four experimental factors—field structure with three levels (full field, left hemi-field, right hemi-field), flow type with two levels (radial, planar), probe position with two levels (-3° , 3°), and probe direction with three levels (75° , 90° , 105°). Similar to Experiment 1, in trials containing the planar flow, dots always moved rightwards (consistent with a leftwards eye or, to a first approximation, head rotation). We measured perceived probe direction and relative tilt. Participants saw each condition eight times leading to 144 trials in total.

Procedure

The procedure was similar to that outlined for Experiment 1.

Data processing and analysis—The preliminary data processing and analysis were similar to those outlined for Experiment 1. Relative tilt was calculated in the same manner as in Experiment 1 and the effects were made commensurate across probe directions using Equation 1. In addition, conditions were labeled both, same, and opposite using the same approach as in Experiment 1.

Relative tilt effects from Experiment 1 were modeled as a weighted linear combination of the effects seen for the individual flow fields in the present experiment. From the relative tilt data seen in the six conditions of Experiment 1 (Figure 8) we constructed the vector:

$$t_{OFI} = (t_B^{-3}, t_B^3, t_S^{-3}, t_S^3, t_O^{-3}, t_O^3)^T,$$

where the subscript in each component refers to the condition type (both, same, opposite) and the superscript refers to the probe position (-3° , 3°). We then constructed an array from the relative tilt data obtained in the present experiment (presented in the following results section)

$$A = \begin{pmatrix} -t_B^R & t_B^P \\ t_B^R & t_B^P \\ -t_S^R & t_S^P \\ t_S^R & t_S^P \\ -t_O^R & t_O^P \\ t_O^R & t_O^P \end{pmatrix},$$

where the subscript in each component corresponds to the field condition (both, same, opposite) and the superscript refers to the flow type condition (radial, planar). Note that the negative signs in Matrix A reflect our implicit assumption that the relative tilts for the radial flow conditions in which the probe is on opposite sides of the field should be opposite in

sign. Based on the data obtained (not shown) this is not an unreasonable assumption.

Finally, using Equation 2, we recover the best fitting weights, $\hat{w} = (\hat{w}^R, \hat{w}^P)^T$, such that

$$\hat{w} = \operatorname{argmin}_w \{ \| t_{OFI} - Aw \| \}, \quad (2)$$

where w^R and w^P denote the weights associated with the radial and planar flow fields, respectively.

We fitted two models. The first had two free parameters w^R and w^P which were unconstrained. This model was used to investigate whether the effects in Experiment 1 might be approximated as either the sum or the difference of the effects seen in Experiment 2; i.e., consistent with what might be predicted from the middle and right columns of Figure 5 which, respectively, reflect global subtraction of either a vector sum or vector difference (radial minus planar) of the flow fields comprising the OFI stimulus. In the former case the weights obtained would be $w^R = 1$, $w^P = 1$, whereas in the latter case the weights would be $w^R = 1$, $w^P = -1$. Alternatively, the effects in Experiment 1 might be approximated as an average $w^R = 0.5$, $w^P = 0.5$.

The second model had only one free parameter w^R and was constrained such that the weight parameters (w^R , w^P) summed to 1 and were in the range [0, 1]. This model was used to investigate whether the effects in Experiment 1 might be approximated as a weighted average of the effects in Experiment 2. We tested whether this one parameter model resulted in a significantly worse fit than the two parameter model using a chi-square difference test.

Results

The average (over observer) relative tilts obtained in the planar and radial flow conditions are shown in Figure 9. Consistent with previous results the relative tilt in the radial flow condition was directed towards the FOE, an effect which was reduced but still persisted when the flow and probe were in opposite hemi-fields (Warren & Rushton, 2009a). A two-factor repeated measures ANOVA conducted on this data revealed main effects of field structure, $F(2, 16) = 34.6$, $p < 0.001$, and flow type, $F(1, 8) = 15.4$, $p = 0.004$, but no interaction between these factors, $F(2, 16) = 2.9$, $p = 0.09$.

Table 1 shows the weights and associated root mean square (RMS) error obtained in using Models 1 and 2 to predict the data from Experiment 1 based on the individual flow field data in Figure 9. Looking at the weights for Model 1, which were unconstrained, we see that although there is variability between observers, they are primarily positive and have absolute magnitude less than one (one exception in each case). The fact that the weights are primarily positive suggests that the data in Experiment 1 are not well fit as the difference between the effects seen in Experiment 2 and instead look like a weighted sum. The weights obtained for the composite observer (i.e., when the data in each condition was averaged over participants before performing the fit) were $\hat{w} = (0.647, 0.574)^T$.

Turning to the weights obtained for Model 2, we see that although there is individual variability between observers, five of the nine have weights which are within 0.06 of $\hat{w}_{avg} = (0.5, 0.5)^T$. The weights obtained for the composite observer are $\hat{w} = (0.599, 0.401)^T$. A chi-square difference test indicated that Model 2, with only one free parameter, did not provide a significantly worse fit to the data and so for the sake of parsimony should be preferred over Model 1. Using these weights the model is seen to predict the data from Experiment 1 well (Figure 8, circles). Taken together, this analysis suggests that the data in Experiment 1 is well modeled as a weighted average of effects seen in Experiment 2 and that the weights are relatively close to equal.

Discussion

Summary

When planar and radial optic flow fields are viewed simultaneously a characteristic illusion in the perceived direction of heading is observed. The perceived heading direction (FOE) is biased in the same direction as that of the planar flow field (Figure 6). We investigated whether the flow parsing process was prone to the same optic flow illusion. By placing a probe into the OFI stimulus we were able to assess whether the perceived trajectory of the probe was consistent with global subtraction of a field with shifted FOE as is obtained in the OFI. We found that the perceived trajectory was not consistent with subtraction of such a perceived heading field (Figure 8). The flow parsing mechanism does not appear to be susceptible to the OFI. In fact the perceived probe trajectory looked rather similar to what might be expected after global subtraction of the field obtained by weighted vector averaging (and therefore summation) of the overlaid fields in the OFI stimulus (Table 1). These results suggest that flow parsing does not necessarily depend on prior estimation of heading.

Optic flow processing for heading estimation and flow parsing—The results of our study raise interesting possibilities for the organization of optic flow processing in the human brain. First it may be the case that processing undertaken to support a perception of heading and that undertaken to support the assessment of scene-relative object movement are entirely separate. This does not seem like a particularly efficient way of implementing the solution to two closely related problems depending fundamentally on recovery of information about self movement. However, it is entirely possible that there are other constraints upon, or other roles for, optic flow processing of which we are currently unaware. It may be the case that the most efficient way to satisfy such constraints and fulfill these roles promotes independence in processing.

A second possibility is that whilst there may be some overlap in processing, the flow parsing process does not use the self-movement information recovered from the heading process directly. For example it may be the case that the initial stages of optic flow analysis are shared but that the analysis undertaken to support flow parsing is supplemented by further information necessary for estimation of scene-relative object movement (e.g., top down information about scene stability).

A third possibility is that the primary aim of optic flow processing is to support flow parsing so that object movement can be isolated (and potentially this is the main reason that the brain exhibits sensitivity to optic flow). Under this account, heading is estimated only *after* flow parsing has been undertaken. This idea is, at least, partially consistent with an argument made by Fajen and Matthis (2011) suggesting that guidance of locomotion requires that the visual system first recovers the object motion component of optic flow. However, we would argue that the functional role of this process is simply to provide knowledge about the movement of objects in the scene, not necessarily to enable guidance of locomotion.

There is some limited evidence against the idea that object movement is estimated before heading based on the presence of small biases in perceived heading when there are moving objects in the field (e.g., Royden & Hildreth, 1996). However, these biases are small and have only been demonstrated for a rather specific set of circumstances in which stimuli do not contain stereo information and are composed of dots. In addition the biases only arise for specific object trajectories and when the moving object fills a large portion of the scene (e.g., Royden & Hildreth, 1996).

A fourth possibility is that optic flow processing is not used in the visual guidance of locomotion (see Rushton, Harris, Lloyd, & Wann, 1998). In this account observers are able to report heading simply because self-movement is estimated as part of other processes (flow parsing, image stabilization, postural control, etc.).

Relation to previous work on the optic flow illusion—There is debate in the literature about the cause of the OFI (Duffy & Wurtz, 1993; Meese, Smith, & Harris 1995; Duijnhouwer et al., 2006); however, two theories are particularly prevalent. In the case of Duffy and Wurtz (1993) it is suggested that the planar flow is interpreted as the sensory consequence of an eye movement (a re-afferent signal). As a consequence the brain attempts to compensate for this and essentially subtracts the planar flow field from the radial field leading to the observed shift in the FOE location. In contrast Meese et al. (1995) suggest that the shift in FOE is nothing more than an instantiation of Dunker's illusion (Dunker, 1929) induced by the planar flow field and acting upon the dots in the radial field.

The aim of this study was not to understand the cause of the OFI illusion, and we do not claim to do so. However, it is interesting to note that if the induced motion account of Meese et al. (1995) was correct then we might have expected to find a simple bias in the perceived probe trajectory in the direction opposite to the planar flow irrespective of the probe location. Our data could be construed as providing some preliminary evidence against this account.

Relation to previous work on flow parsing—In Warren and Rushton (2008) we investigated perceived trajectory of a probe moving vertically upwards from the center of a radial flow field. We manipulated the number of dots in the left and right hand hemi-fields as well as the amount of noise in the display which was determined by shuffling the location (but not the motion trajectory) of a proportion of dots in the field. In one condition the vast majority of dots were on the right hand side of the field and 50% of the dots were shuffled in location (within hemi-field). This had the effect of producing a stimulus which was similar to that used in Experiment 1 in the right hemi-field condition with the shuffled dots taking the place of the planar flow in the present experiment. The difference is that in the previous experiment the probe was always at the center of the display and the shuffled dots, although predominantly moving to the right, also had a random vertical component (which approximately summed to zero over the hemi-field). In this condition the probe was seen to tilt significantly to the left (i.e., away from the hemi-field containing the majority of the flow). This finding is consistent with the pattern of results seen here (see Figure 8).

Conclusions

Optic flow processing supports a number of roles for the active observer. Some have suggested that the most important of these is the estimation of heading information for the guidance of locomotion (although see Rushton et al., 1998). Recently a new important role for optic flow processing has been suggested in the assessment of scene-relative object movement information. Although the mechanisms required to underpin these roles must rely on similar information, our data lead us to believe that flow parsing for assessment of object movement probably does not depend on a prior estimate of heading.

Supplementary Material

Refer to Web version on PubMed Central for supplementary material.

Acknowledgments

This work was supported by the Wellcome Trust [89934] (PAW, SKR). We thank two anonymous reviewers for their comments on earlier versions of this paper.

References

- Bravo MJ. A global process in motion segregation. *Vision Research*. 1998; 38:853–863. [PubMed: 9624435]
- Calabro F, Soto-Faraco S, Vaina L. Acoustic facilitation of object movement detection during self-motion. *Proceedings of the Royal Society B: Biological Sciences*. 2011; 278:2840–2847.
- Champion RA, Freeman TCA. Discrimination contours for the perception of head-centered velocity. *Journal of Vision*. 2010; 10(6):14, 1–9. doi:10.1167/10.6.14. <http://www.journalofvision.org/content/10/6/14> [PubMed: 20884563]
- Duffy CJ, Wurtz RH. An illusory transformation of optic flow fields. *Vision Research*. 1993; 33:1481–1490. [PubMed: 8351820]
- Duijnhouwer J, Beintema JA, van den Berg AV, van Wezel RJA. An illusory transformation of optic flow fields without local motion interactions. *Vision Research*. 2006; 46:439–443. [PubMed: 16009393]
- Dunker K. Über induzierte Bewegung (Ein Beitrag zur Theorie optisch wahrgenommener Bewegung) [Concerning induced movement (A contribution to the theory of visually perceived movement)]. *Psychologische Forschung*. 1929; 12:180–259.
- Donaldson I. The functions of the proprioceptors of the eye muscles. *Philosophical Transactions of the Royal Society of London. Series B: Biological Sciences*. 2000; 355:1685–1754.
- Fajen B, Matthis J. Visual and non-visual contributions to the perception of object motion during self-motion. *Journal of Vision*. 2011; 11(11):920. doi:10.1167/11.11.920. <http://www.journalofvision.org/content/11/11/920>
- Frost B, Nakayama K. Single visual neurons code opposing motion independent of direction. *Science*. 1983; 220:744–745. [PubMed: 6836313]
- Gibson, JJ. *The perception of the visual world*. Houghton Mifflin; Boston, MA: 1950.
- Lappe M, Pekel M, Hoffman KP. Optokinetic eye movements elicited by radial optic flow in the macaque monkey. *Journal of Neurophysiology*. 1998; 79:1461–1480. [PubMed: 9497425]
- Matsumiya K, Ando H. World-centered perception of 3D object motion during visually guided self-motion. *Journal of Vision*. 2009; 9(1):15, 1–13. doi:10.1167/9.1.15. <http://www.journalofvision.org/content/9/1/15> [PubMed: 19271885]
- Meese TS, Smith V, Harris MG. Induced motion may account for the illusory transformation of optic flow fields found by Duffy and Wurtz. *Vision Research*. 1995; 35:981–984. [PubMed: 7762154]
- Miles FA, Kawano K, Optican LM. Short-latency ocular following responses of monkey. I. Dependence on temporospatial properties of visual input. *Journal of Neurophysiology*. 1986; 56:1321–1354. [PubMed: 3794772]
- Niemann T, Lappe M, Büscher A, Hoffman KP. Ocular responses to radial optic flow and single accelerated targets in humans. *Vision Research*. 1999; 39:1359–1371. [PubMed: 10343848]
- Royden CS, Hildreth EC. Human heading judgments in the presence of moving objects. *Perception & Psychophysics*. 1996; 58:836–856. [PubMed: 8768180]
- Royden CS, Connors EM. The detection of moving objects by moving observers. *Vision Research*. 2010; 50:1014–1024. [PubMed: 20304002]
- Royden CS, Wolfe JM, Klempen N. Visual search asymmetries in motion and optic flow fields. *Perception and Psychophysics*. 2001; 63:436–444. [PubMed: 11414131]
- Rushton SK, Bradshaw MF, Warren PA. The pop out of scene-relative object movement against retinal motion due to self-movement. *Cognition*. 2007; 105:237–245. [PubMed: 17069787]
- Rushton SK, Harris JM, Lloyd MR, Wann JP. Guidance of locomotion on foot uses perceived target location rather than optic flow. *Current Biology*. 1998; 8:1191–1194. [PubMed: 9799736]
- Rushton SK, Warren PA. Moving observers, relative retinal motion and the detection of object movement. *Current Biology*. 2005; 15:R542. [PubMed: 16051158]

- Sperry R. Neural basis of the spontaneous optokinetic response produced by visual inversion. *Journal of Comparative and Physiological Psychology*. 1950; 43:482–489. [PubMed: 14794830]
- van den Berg A. Robustness of perception of heading from optic flow. *Vision Research*. 1992; 32:1285–1296. [PubMed: 1455703]
- von Holst, E.; Mittelstaedt, H. *Selected Papers of Erich von Holst: The Behavioural Physiology of Animals and Man*. Martin, R., translator. Methuen; London: 1950. p. 39-73. From German
- Warren WH, Morris MW, Kalish M. Perception of translational heading from optical flow. *Journal of Experimental Psychology: Human Perception and Performance*. 1988; 14:646–660. [PubMed: 2974874]
- Warren PA, Rushton SK. Perception of object trajectory: Parsing retinal motion into self and object movement components. *Journal of Vision*. 2007; 7(11):2, 1–11. doi:10.1167/7.11.2. <http://www.journalofvision.org/content/7/11/2> [PubMed: 17997657]
- Warren PA, Rushton SK. Evidence for flow-parsing in radial flow displays. *Vision Research*. 2008; 48:655–663. [PubMed: 18243274]
- Warren PA, Rushton SK. Optic flow processing for the assessment of object movement during ego movement. *Current Biology*. 2009a; 19:1555–1560. [PubMed: 19699091]
- Warren PA, Rushton SK. Perception of scene-relative object movement: Optic flow parsing and the contribution of monocular depth cues. *Vision Research*. 2009b; 49:1406–1419. [PubMed: 19480063]

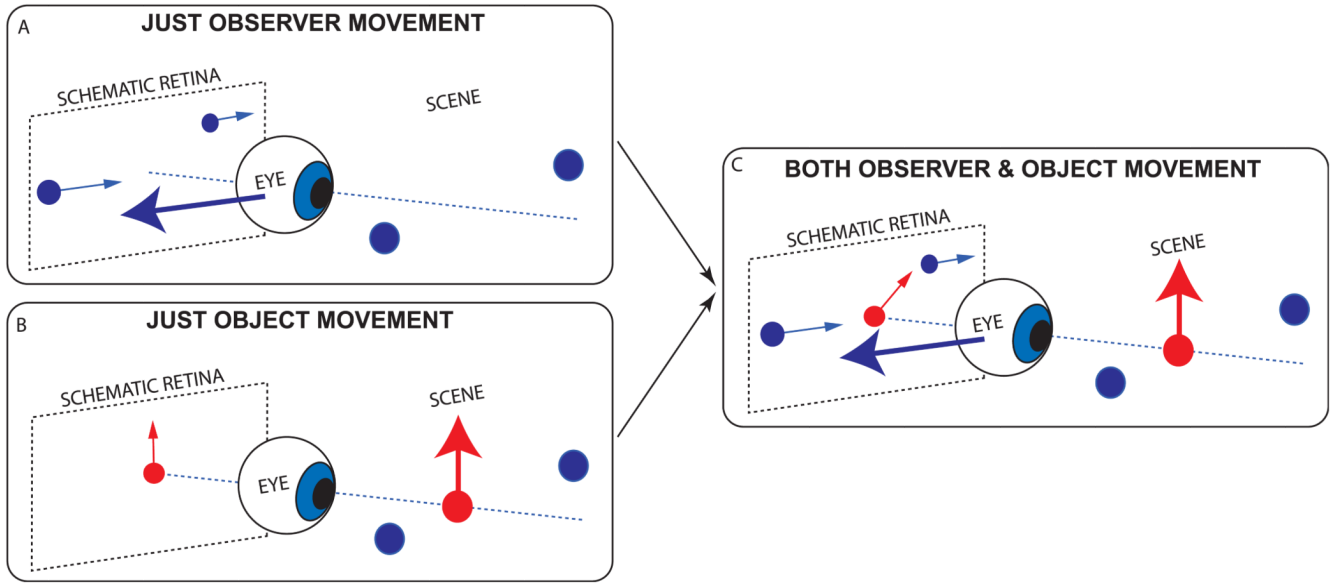


Figure 1. Schematic illustration of the problem of recovering an appropriate estimate of scene-relative object movement when an observer is moving. Retinal motion occurs when (A) the scene is stationary but the object moves; (B) the observer is stationary but an object moves in the scene; or (C) The observer moves and there are both stationary and moving objects in the scene.

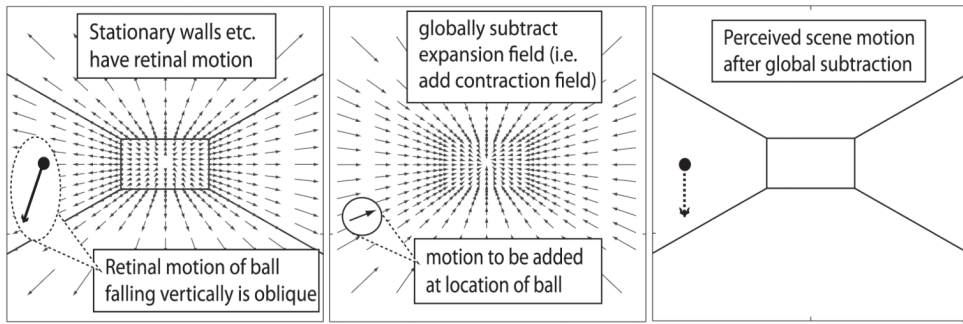


Figure 2. Schematic illustration of the flow parsing hypothesis (reproduced from Warren & Rushton, 2009b).

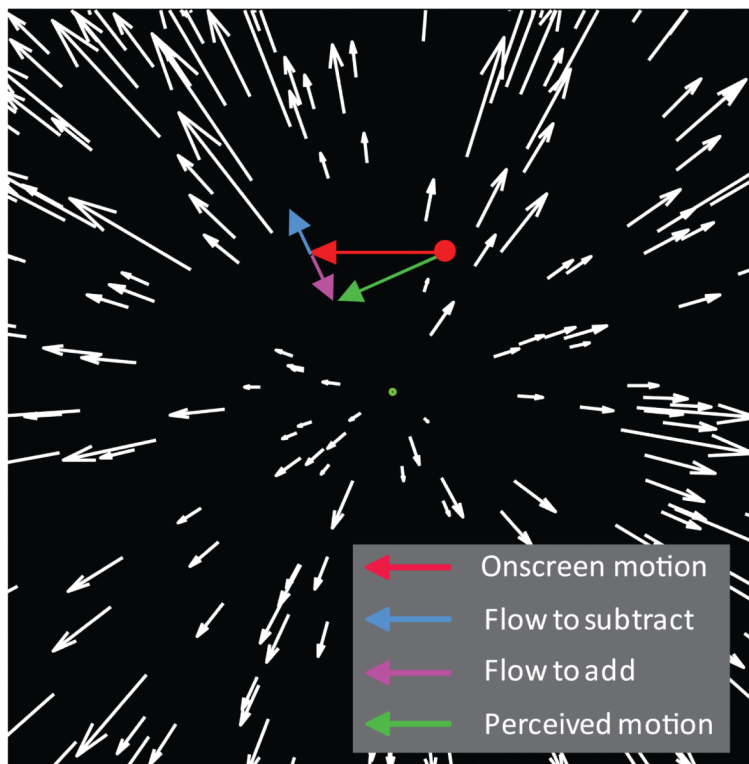


Figure 3. Schematic illustration of a stimulus used in Warren and Rushton (2009a). In one condition observers viewed a dot moving horizontally across a radial flow field (red) above a central fixation spot aligned with the FOE of the flow. Under flow parsing the brain subtracts a global radial component which at the location of the dot is represented by the blue motion vector. Subtraction of the blue vector is equivalent to addition of the magenta vector. Vector addition of the physical (red) component and that arising due to the subtraction process (magenta) then gives the resultant perceived motion (green).

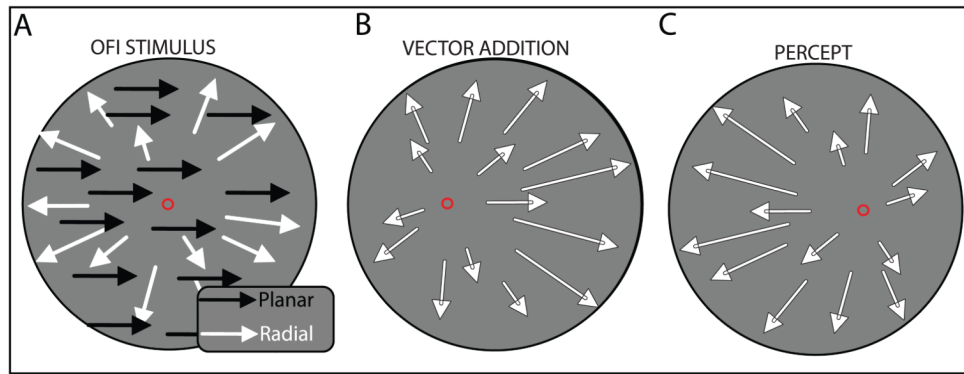


Figure 4. Schematic illustration of the OFI stimulus (A) together with possible percepts involving vector addition (B) or subtraction (C) of the components of the OFI stimulus. Surprisingly, when viewing (A) observers tend to perceive a shift in FOE consistent with (C).

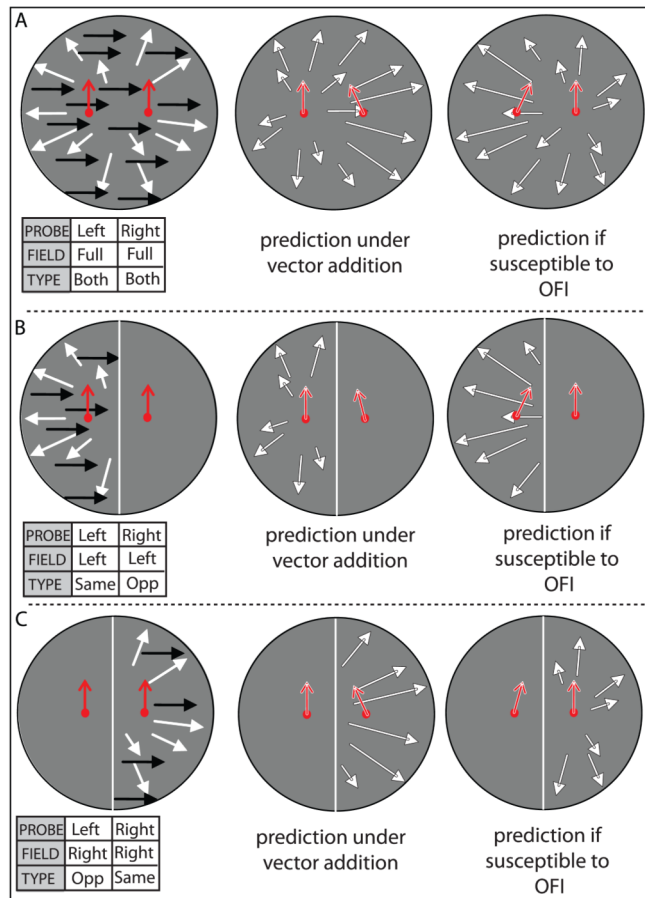


Figure 5. Schematic illustration of the OFI stimuli used in Experiment 1 (left panels) and possible outcomes for perceived probe trajectory (middle and right panels). Different combinations of probe position and field structure are labeled in the tables below the stimuli. In each table the row marked probe defines the probe position condition and the row marked field defines the field condition. The row marked type then defines the condition type (see Data processing and analysis section for further information). So, for example, in the left panel of Figure 5B the condition illustrated in which the probe is on the right and the flow is in the left hemi-field is an opposite type condition. For both sets of predictions the onscreen probe motion is drawn in red and the predicted perceived motion is drawn in red with a dotted white outline. In the middle column, predictions are consistent with subtraction of a flow field (illustrated by white arrows) similar to that obtained by vector addition of the overlaid flow fields in the OFI stimulus. Predictions in the right column are consistent with subtraction of a flow field similar to that obtained under the OFI (illustrated by white arrows).

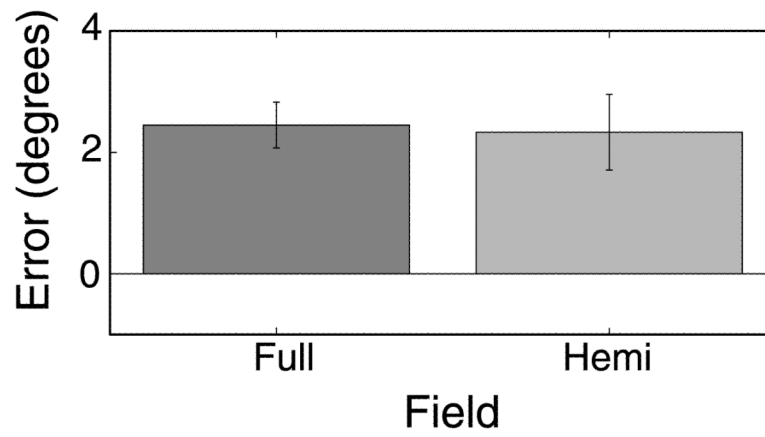


Figure 6. Data from the Preliminary experiment averaged over participants, revealing a clear bias in the perceived heading direction. Positive errors correspond to shifts in the FOE in the direction of the planar flow field. The effect appears to be similar irrespective of whether the full field or hemi-field of flow is presented. Error bars represent \pm SE.

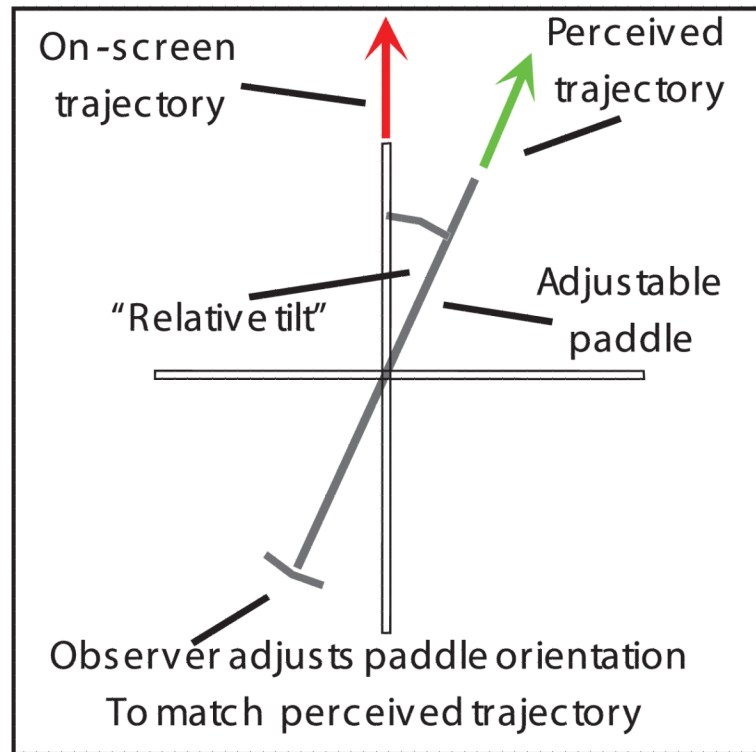


Figure 7. The adjustable gauge used in Experiments 1 and 2.

The red arrow indicates a possible onscreen trajectory for the probe (in this case vertically upwards) and the green arrow indicates the trajectory perceived by the observer. The observer is asked to set the orientation of an adjustable paddle to match the orientation of the perceived probe trajectory.

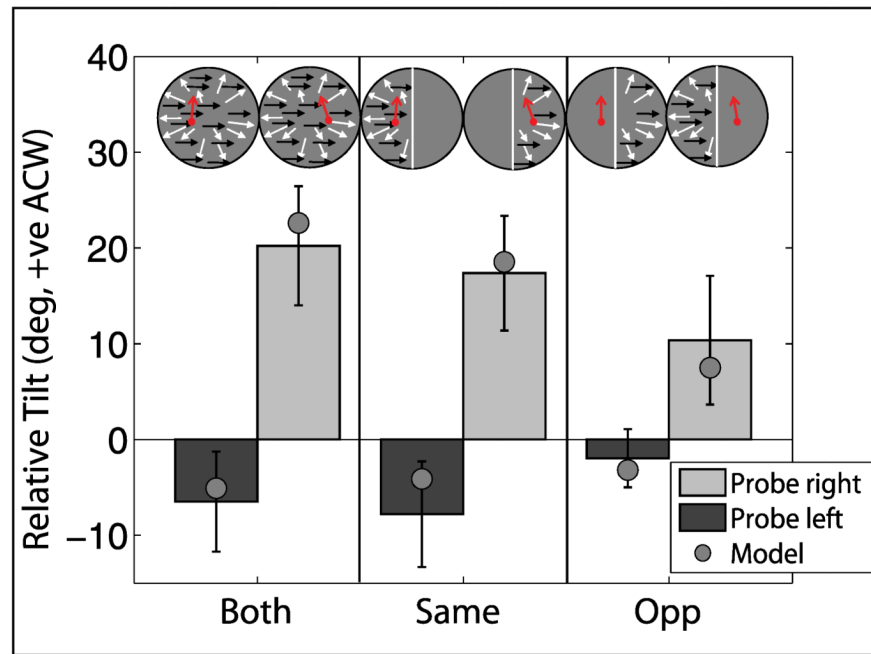


Figure 8. Data from Experiment 1.

Light bars show data from conditions in which the probe was in the right hemi-field. Dark bars show data from conditions in which the probe was in the left hemi-field. Circles correspond to the best fit linear weighting model described after Experiment 2. Relative tilt is measured as positive in the anticlockwise (ACW) direction. Error bars represent 95% confidence intervals. A schematic illustration of the conditions together with a graphical representation of the effects (orientation of red arrow relative to vertical) is also provided at the top of the plot.

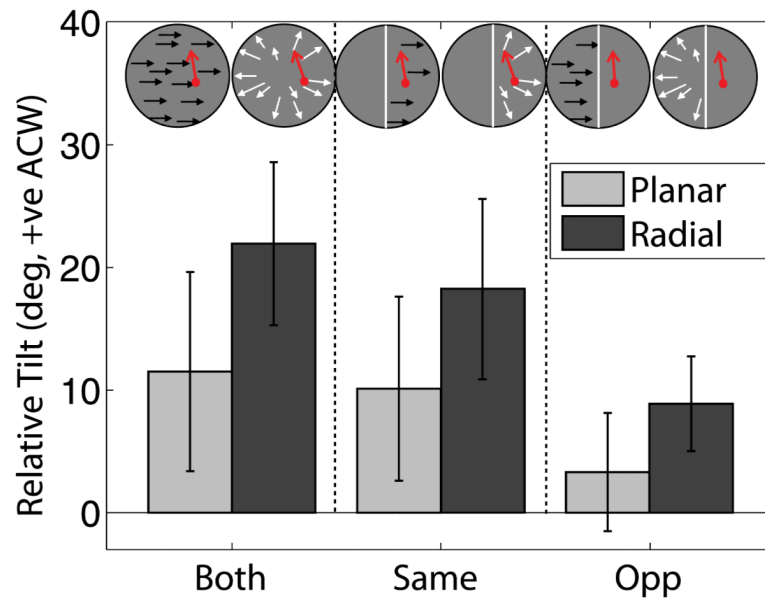


Figure 9. Data from Experiment 2.

Relative tilts obtained for the pure planar and radial flow fields. Light and dark bars show data from conditions in which stimulus contained only planar and radial flow, respectively. All data are presented as if the probe was always in the right hemi-field. Error bars represent 95% confidence intervals. A schematic illustration of the conditions together with a graphical representation of the effects (orientation of red arrow relative to vertical) is also provided at the top of the plot.

Table 1
Best fitting weights and associated χ^2 values recovered by fitting Models 1 and 2 to the data in Experiments 1 and 2.

Weights are shown for all nine observers individually together with the fit obtained when data was averaged over observers to form the composite observer before fitting. Note in Model 2 that the weights are constrained to sum to 1. In the final two rows we compare models using a χ^2 difference test.

	P1	P2	P3	P4	P5	P6	P7	P8	P9	COMP
Model 1										
R	0.584	0.915	0.708	0.507	0.575	0.666	0.889	0.460	0.504	0.647
P	0.817	0.261	0.117	1.654	0.797	-0.223	0.422	0.255	0.570	0.574
χ^2	0.699	0.482	0.330	0.436	0.135	0.201	0.806	0.544	0.217	0.417
Model 2										
R	0.512	0.818	0.731	0.381	0.446	0.987	0.855	0.521	0.470	0.599
P	0.488	0.182	0.269	0.619	0.554	0.013	0.145	0.479	0.530	0.401
χ^2	1.507	1.199	0.462	1.637	1.732	0.692	0.833	1.318	0.367	0.993
Comparison—Model 2 vs. Model 1										
$\chi^2(1)$	0.808	0.717	0.132	1.201	1.598	0.491	0.027	0.774	0.150	0.576
<i>p</i>	0.144	0.310	0.637	0.262	0.174	0.221	0.630	0.208	0.724	0.377